Journal of Controlled Release 244 (2016) 41–51

Contents lists available at ScienceDirect

Journal of Controlled Release

journal homepage: www.elsevier.com/locate/jconrel

Controlling drug release from non-aqueous environments: Moderating delivery from ocular silicone oil drug reservoirs to combat proliferative vitreoretinopathy

Helen Cauldbeck [a], Maude Le Hellaye [a,b], Mark Long [c], Stephnie M. Kennedy [b], Rachel L. Williams [b], Victoria R. Kearns [b,*], Steve P. Rannard [a,*]

[a] Department of Chemistry, University of Liverpool, Crown Street, L69 7ZD, UK
[b] Department of Eye and Vision Science, University of Liverpool, Liverpool, UK
[c] Unilever Research Centre, Port Sunlight, Quarry Road East, Bebington, Wirral CH63 3JW, UK

ARTICLE INFO

Article history:
Received 24 August 2016
Received in revised form 5 November 2016
Accepted 10 November 2016
Available online 12 November 2016

Keywords:
Hydrogen bonding
Non-polar drug reservoir, ocular drug delivery
Silicone oil
Graft copolymer
RAFT polymerization

ABSTRACT

In a number of cases of retinal detachment, treatment may require the removal of the vitreous humour within the eye and replacement with silicone oil to aid healing of the retina. The insertion of silicone oil offers the opportunity to also deliver drugs to the inside of the eye; however, drug solubility in silicone oil is poor and release from this hydrophobic drug reservoir is not readily controlled. Here, we have designed a range of statistical graft copolymers that incorporate dimethylsiloxane and ethylene glycol repeat units within the side chains, allowing short chains of oligo(ethylene glycol) to be solubilised within silicone oil and provide hydrogen bond acceptor sites to interact with acid functional drug molecules. Our hypothesis included the potential for such interactions to be able to delay/control drug release and for polymer architecture and composition to play a role in the silicone oil miscibility of the targeted polymers. This strategy has been successfully demonstrated using both ibuprofen and all-trans retinoic acid; drugs with anti-inflammatory and anti-proliferation activity. After the copolymers were shown to be non-toxic to retinal pigment epithelial cells, studies of drug release using radiochemical approaches showed that the presence of 10 v/v% of a linear graft copolymer could extend ibuprofen release over three-fold (from 3 days to >9 days) whilst the release of all-trans retinoic from the silicone oil phase was extended to >72 days. These timescales are highly clinically relevant showing the potential to tune drug delivery during the healing process and offer an efficient means to improve patient outcomes.

1. Introduction

Retinal detachment is a relatively common disorder requiring urgent attention to prevent the potential for permanent reduction or loss of sight [1]. The incidence of non-traumatic retinal detachment in individuals with healthy eyes may be as low as 5.4 cases/100,000 people per year [2], but correlations with age, genetics [3], race, short-sight (myopia) [4], previous surgical interventions (*e.g.* cataract surgery) and underlying illness, such as diabetes, may increase this figure to >50 cases/100,000 people per year [5,6]. The condition involves the physical separation of the neuroretina from the supporting retinal pigment epithelium (RPE) monolayer, a layer of hexagonally close packed cells situated at the back of the human eye. Upon detachment, and subsequent tearing, of the retina, aqueous from around the vitreous humour may accumulate between the two layers leading to further separation from the RPE; this is known as rhegmatogenous retinal detachment. Retinal detachment may occur without the formation of a tear either by the buildup of fluid under the retina from blood vessels, so called exudative retinal detachment, triggered by conditions such as severe macular degeneration, very high blood pressure or certain cancers such as choroidal melanoma. Alternatively, tractional retinal detachment may occur after scar tissue forms on the surface of the retina and contracts, leading to separation of the retina from the RPE [7]; this process is associated with proliferative diabetic retinopathy and proliferative vitreoretinopathy (PVR). PVR is a known complication of rhegmatogenous retinal detachment and recurring retinal detachment as the formation of a tear in the retina results in the production of an inflammatory microenvironment [8]. Several cell types are stimulated by these cues, in particular RPE cells, which may proliferate and de-differentiate into a macrophage-like phenotype. RPE cells may also undergo epithelial-mesenchymal transition, probably as a result of exposure to a variety of agents in the microenvironment such as members of the transforming growth factor beta and platelet-derived growth factor families [9]. The cells migrate towards the vitreous humour with

* Corresponding authors.
E-mail addresses: vkearns@liverpool.ac.uk (V.R. Kearns), srannard@liverpool.ac.uk (S.P. Rannard).

http://dx.doi.org/10.1016/j.jconrel.2016.11.010

many cells adopting a myofibroblastic phenotype. Cells deposit extracellular proteins, leading to the formation of new tissue. As this tissue matures and is remodeled, it contracts, leading to the formation of a scar. The epiretinal membrane of the scar continues to grow and later contraction leads to further tension and additional retinal detachment [10] with subsequent loss of vision [11].

Therapeutic intervention for retinal detachment includes the use of pneumatic retinopexy, scleral buckle surgery and the combination of vitrectomy/tamponade replacement. Pneumatic retinopexy requires the injection of a gas bubble (air or perfluorocarbon) into the vitreous cavity and careful positioning of the patients' head to align the bubble with the detached area, this generates a light pressure which is able to hold the tear against the RPE. The process takes up to three weeks, during which the gas is slowly absorbed. It also leads to obvious restrictions for the patient including postural and lifestyle limitations [12]. A scleral buckle is a piece of silicone rubber or plastic that is sewn onto the external surface of the eye to permanently deform the sclera towards the detached retina [13]. The buckle may completely surround the eye if large detachments are present [14].

A vitrectomy involves the removal of some or all of the vitreous humour from the eye and replacement with a gas or silicone oil tamponade [15]; a tamponade agent is a material that will plug or compress an area or cavity. The hydrophobic nature of the tamponade inhibits the accumulation of physiological liquids in the subretinal space, excludes inflammatory factors and encourages reattachment. During the use of a gas tamponade, the patient must lie predominantly facing downwards for up to 4 weeks to ensure the gas bubble is aligned with the damaged region and any remaining vitreous material is held away from the repair site as the motion of the viscous fluid may lead to greater damage; again, this is highly restricting to the patient. The use of a silicone oil tamponade (Fig. 1) was reported almost 20 years ago to provide considerable patient benefits over the use of gaseous alternatives [16]. Silicone oil has many benefits for use as a tamponade agent including being chemically inert, readily sterilized and optically clear, which allows at least some vision in most patients [17]. It also allows considerably reduced postural restrictions and the ability to travel during the healing of the retina. Disadvantages include the need to remove the tamponade ultimately and reported cases of elevated intraocular pressure.

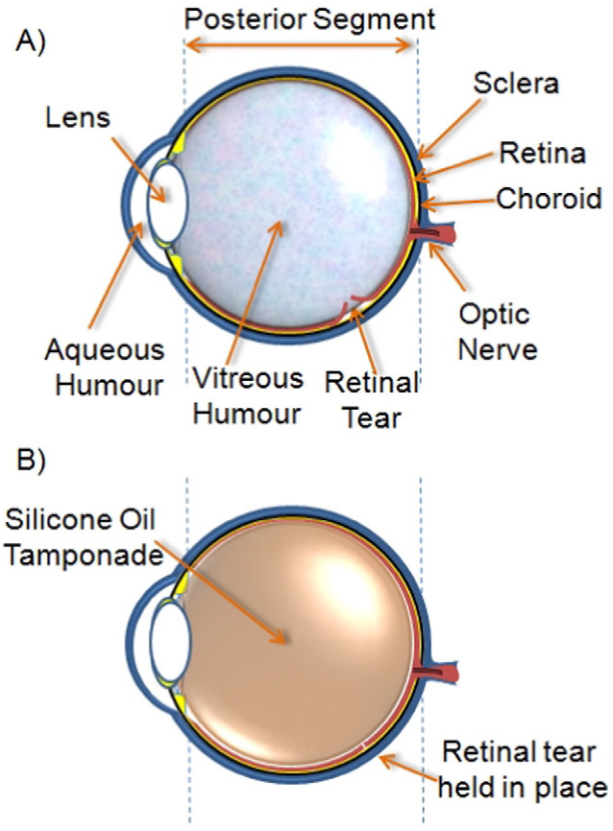

Fig. 1. Schematic cross-section of the a human eye showing A) the formation of a retinal tear; and B) Replacement of the vitreous humour within the eye with a silicone oil tamponade to aid healing of the tear whilst maintaining vision for the patient.

Currently the action of the silicone oil tamponade is predominantly physical and attempts to utilize the volume of injected oil as a drug delivery reservoir have been hampered by either the poor solubility of many drugs within silicone oil or the inability to control release rates. The opportunity has significant clinical relevance as the ability to control the release of anti-proliferative drugs and/or anti-inflammatory agents to the posterior of the eye would present options to considerably extend the therapeutic action of this surgical intervention [18]. Drug delivery from, and into, aqueous environments has been studied by numerous research groups for many years and for many diseases [19], including ocular conditions [20]. Much of the recent research has utilized nanoparticle systems [21,22], supra-molecular assembly [23,24] or polymer-drug conjugation [25,26], with highly efficient targeting of disease sites often reported using *in vitro* and *in vivo* animal models. Many of these reports utilize either the poor water-solubility of the drug compound or a cleavable chemistry to avoid instant/uncontrolled drug release and mediate delivery to the target site. The challenges associated with the development of silicone oil tamponade drug delivery reservoirs include: 1) the poor-solubility of drug compounds within silicone oil, 2) the inherent low solubility of silicone-soluble drugs in water, 3) a restricted range of silicone-soluble/miscible excipient materials to moderate release, and 4) difficulties in directly assessing drug concentrations within the silicone oil phase. Polymer-drug conjugates and nanoparticle delivery strategies have potential within this context, however, the eye is considered as one of the most complex organs with a series of unique barriers that limit fluid transport, and hence drug delivery from conventional topical or systemic routes; the eye is isolated by the blood-retinal and blood-aqueous barriers [27]. The presence of residual nanoparticles, degradation products and cleaved polymer carriers leads to the potential for localized toxicity, especially with the constraints of clearance/transport from the posterior of the eye.

Herein we describe the design, synthesis and *in vitro* evaluation of a new strategy for moderating drug delivery from silicone oil tamponades. The approach involves the formation of silicone oil soluble/miscibile polymeric excipients that are able to hydrogen bond to acid functional drug compounds and alter release rates into aqueous environments. A series of studies using two clinically relevant drugs, and mixtures with ^{3}H-labelled drug compounds, clearly illustrates the clinical potential for this novel approach.

2. Materials and methods

2.1. Materials

All-trans retinoic acid (atRA) was purchased from Xian Bosheng Biological Technology Co., Ltd. and used as received. Ibuprofen (Ibu) was purchased from Tokyo Chemical Industry UK Ltd. and used as received. Trimethylsiloxy terminated polydimethylsiloxane oil (silicone oil; SiO_{1000}; viscosity = 900–1200 cSt at 25 °C) was donated by Fluoron GmbH and used as received. All deuterated solvents were purchased from Sigma-Aldrich and used as received apart from $CDCl_3$ where 0.1% TMS was added. All solvents used were analytical grade and purchased from Fisher. Resazurin was purchased from Sigma and used as received. Alexa Fluor® 488 Phalloidin (Phalloidin) and 4′,6-diamidino-2-phenylindole dihydrochloride (DAPI) were purchased from Invitrogen and diluted in methanol or deionized water following the manufacturer's instructions. Adult retinal pigment epithelial (ARPE-19) cells were bought from American Type Culture Collection, Manassas, VA, USA, catalogue number CRL 2302 and frozen stocks were stored in-house. Dulbecco's Modified Eagle Medium/Ham's Nutrient Mixture

F-12 Formulation (DMEM/F12, catalogue number D8437), Penicillin Streptomycin 10 mg/mL streptomycin in 0.9% NaCl (Pen-Strep), Amphotericin B solution 250 μg/mL in deionized water, Dulbecco's calcium and magnesium free phosphate buffered saline (PBS), Trypsin-EDTA containing 5 g porcine trypsin and 2 g ethylenediaminetetraacetic acid (Trypsin) and neutral buffered formalin (NBF) were purchased from Sigma-Aldrich and used as received. Fetal bovine serum (FCS) was purchased from BioSera and used as received. All tissue culture plates and flasks were purchased from Greiner, except black 96 well plates which were purchased from Costar. Poly (ethylene glycol) methyl ether methacrylate ($M_n = 300\ gmol^{-1}$) (98%) (OEGMA), 2-cyano-2-propyl benzodithioate (97%) (CPBD) and 2.2′-azobis(2-methylpropionitrile) (98%) (AIBN) were purchased from Sigma-Aldrich and used as received. Mono methacryloxypropyl poly(dimethylsiloxane) methacrylate (molecular weight 985 and 4600 $gmol^{-1}$; $PDMSMA_9$ and $PDMSMA_{57}$ respectively) and methacryloxypropyl poly(dimethylsiloxane) dimethacrylate (molecular weight 1275 and 4460 $gmol^{-1}$; $PDMSDMA_{12}$ and $PDMSDMA_{55}$ respectively) were purchased from Gelest and used as received.

2.2. Characterization

NMR spectra were recorded using a Bruker DPX-400 spectrometer operating at 400 MHz for ^1H NMR. UV–vis spectra were collected using a Thermo Fisher NanonDrop 2000c spectrophotometer with a quartz cuvette. Data was analyzed using the NanoDrop2000 software. ProSafe + scintillation cocktail (Meridian Biotechnologies Ltd.) was used as received. All radiation measurements were carried out using a liquid scintillation counter (Packard Tri-carb 3100TR; Isotech). Triple detection GPC was performed to measure molecular weights and molecular weight distributions using a Malvern Viscotek instrument. The instrument was equipped with a GPCmax VE2001 autosampler, two Viscotek T6000 columns (and a guard column), a refractive index (RI) detector VE3580 and a 270 Dual Detector (light scattering and viscometer) with a mobile phase of THF containing 2 v/v% of trimethylamine at 35 °C with a flow rate of 1 mL min^{-1}. A Nikon Eclipse Ti-E inverted microscope system was used to collect cell images. Statistical analyses were carried out on SPSS Statistics V22 software; one way test of homogeneity of variances and ANOVA as well as Dunnett's T3 post-hoc evaluation were conducted, $p < 0.05$ was regarded to be statistically significant.

2.3. Synthesis of polymers

All RAFT polymerizations were conducted at a constant ratio of chain transfer agent to initiator of [CPBD]:[AIBN] = 1:0.2.

For the synthesis of *p*(OEGMA), targeting $DP_n = 60$ monomer units, AIBN (2.7 mg, 0.016 mmol), CPBD (18.4 mg, 0.083 mmol) and OEGMA (1.5 g, 5 mmol) were added to a 25 mL Schlenk tube equipped with a magnetic stirrer bar. ^{t}-BuOH (4.5 mL, 30 wt% wrt. monomer, deoxygenated *via* N_2 purge) was added and the resulting solution degassed by five cycles of freeze/pump/thaw. After the final thaw cycle, the flask was backfilled with N_2. The reaction flask was placed into a pre-heated oil bath (70 °C) and stirred for 8 h, after which the reaction medium was observed to be slightly turbid. The polymerization was stopped by cooling the flask to ambient temperature, exposing its contents to air and diluting the reaction medium with ^{t}-BuOH. The solution was concentrated by rotary evaporation and precipitated into cold petroleum-ether (40–60) to give a pink liquid. The sample was dried under vacuum at 40 °C for 24 h and analyzed by ^1H NMR in $CDCl_3$ and GPC with a mobile phase of THF.

In a typical synthesis of *p*(OEGMA-*stat*-$PDMSMA_9$), targeting $DP_n = 60$ monomer units (OEGMA/$PDMSMA_9$ 50/50), AIBN (2.7 mg, 0.016 mmol), CPBD (18.4 mg, 0.083 mmol), OEGMA (0.148 g, 0.492 mmol) and $PDMSMA_9$ ($M_n = 985\ gmol^{-1}$, 1.5 g, 1.524 mmol) were added to a 25 mL Schlenk tube equipped with a magnetic stirrer bar. ^{t}-BuOH (4.96 mL, 30 wt% wrt. monomer, deoxygenated *via* N_2 purge) was added and the resulting solution degassed by five cycles of freeze/pump/thaw. After the final thaw cycle, the flask was backfilled with N_2. The reaction flask was placed into a pre-heated oil bath (70 °C) and stirred for 24 h, after which the reaction medium was observed to be slightly turbid. The polymerization was stopped by cooling the flask to ambient temperature, exposing its contents to air and diluting the reaction medium with ^{t}-BuOH. The solution was concentrated by rotary evaporation and precipitated into cold MeOH to give a pink liquid. The sample was dried under vacuum at 40 °C for 24 h and analyzed by ^1H NMR in $CDCl_3$ and GPC with a mobile phase of THF.

In a typical branched polymerization synthesis of *p*(OEGMA-*stat*-$PDMSMA_9$-*stat*-$PDMSDMA_{12}$), targeting $DP_n = 60$ monomer units (OEGMA/$PDMSMA_9$ 50/50), AIBN (5.6 mg, 0.034 mmol), CPBD (37.5 mg, 0.169 mmol), OEGMA (1.524 g, 5 mmol), $PDMSMA_9$ ($M_n = 985\ gmol^{-1}$, 5 g, 5 mmol) and $PDMSDMA_{12}$ ($M_n = 1275\ gmol^{-1}$, 0.205 g, 0.158 mmol) were added to a 100 mL Schlenk tube equipped with a magnetic stirrer bar. ^{t}-BuOH (20.3 mL, 30 wt% wrt. monomer, deoxygenated *via* N_2 purge) was added and the resulting solution degassed by five cycles of freeze/pump/thaw. After the final thaw cycle, the flask was backfilled with N_2. The reaction flask was placed into a pre-heated oil bath (70 °C) and stirred for 24 h, after which the reaction medium was observed to be slightly turbid. The polymerization was stopped by cooling the flask to ambient temperature, exposing its contents to air and diluting the reaction medium with ^{t}-BuOH. The solution was concentrated by rotary evaporation and precipitated into MeOH to give a pink liquid. The sample was dried under vacuum at 40 °C for 24 h and analyzed by ^1H NMR spectroscopy in $CDCl_3$ and GPC with a mobile phase of THF.

CTA removal involved a ratio of polymer:AIBN = 1:20. In a typical CTA removal *p*($PDMS_{(9)48}$-*stat*-$OEGMA_{12}$) (5.3811 g, 0.112 mmol) was dissolved in toluene (73 mL, deoxygenated *via* Ar purge) in a 100 mL schlenk flask equipped with a stirrer bar. AIBN (369 mg, 2.24 mmol) was added to the reaction flask and purged with Ar. The temperature was raised to 80 °C for 2.5 h. After the reaction with AIBN, the polymer was precipitated in cold MeOH and a white liquid was isolated by decanting the MeOH. The product was dried *in vacuo* then analyzed by ^1H NMR spectroscopy in $CDCl_3$.

2.4. Solubilization/miscibility studies of polymers in silicone oils

In a typical solubilization experiment, polymer (1 mL) and silicone oil (SiO_{1000}; 1 mL) were syringed into a glass vial to create a 50 v/v% mixture and placed on a roller for 3 days. The solutions were diluted systematically by adding silicone oil to decrease the amount of polymer by 10 v/v%, rolled for 3 days each time, until a soluble/miscible concentration was reached (*i.e.* 40, 30, 20, 10 also 5 and 1 v/v% were tested).

2.5. Radiometric studies and analysis of drug solubility in silicone oils and release

To determine solubility of drugs in silicone oil, saturated solutions of atRA and Ibu in silicone oil (SiO_{1000}) were prepared by mixing atRA (11.6 mg) or Ibu (32 mg) with tritiated versions of the drug (10 μCi) in EtOH (2 mL); after evaporation of the solvent at ambient temperature, SiO_{1000} (5 mL) was added to the residual solid and the solution was stirred for 2 weeks. The sample was filtered using a syringe pump (4 mL/h) and 0.45 μm PTFE filters. Samples of the filtered oils (20 μL) were then solubilised in diethyl ether (8 mL) before scintillation cocktail (10 mL) was added. Radiation was then measured on a scintillation counter and saturation concentrations were determined.

Amounts of drug added to the samples were altered depending on targeted final concentrations. Solutions of 200 μg/mL: atRA (1 mg) and tritiated atRA (6 μCi) were mixed in EtOH (2 mL) and the same protocol was followed. Solutions of 20 μg/mL: atRA (0.1 mg) and tritiated atRA (2 μCi) were mixed in EtOH (2 mL) and the same procedure was carried

out. Solutions of 1 mg/mL: Ibu (5 mg) and tritiated Ibu (7.5 μCi) were mixed in EtOH (2 mL) and the same protocol was followed.

For the preparation of both atRA and Ibu solutions in $p(PDMSMA_{(9)48}$-*stat*-$OEGMA_{12})$ blends, 5 and 10 v/v% content of polymer blends were prepared by mixing for 3 days and loaded with drug by following the same protocols as described above.

To determine release concentrations of drug, 1 mL of silicone oil or $p(PDMSMA_{(9)48}$-*stat*-$OEGMA_{12})$ blend (5 or 10 v/v%) with determined concentration of drug was placed in a 24 well plate over 0.5 mL media (containing 1% Pen-Strep, 1% Amphotericin B and supplemented with 10% FCS). Samples of media (0.5 mL) were taken and replaced at determined time intervals; daily for the first critical week then every 2–3 days for the remainder of the study, using a 1 mL syringe and 25 gauge needle for up to 71 days. Sampling and withdrawing of the media was done very carefully in order to avoid any emulsification of the oil. Media (250 μL) was mixed with scintillation cocktail (10 mL) and analyzed by liquid scintillation counting.

2.6. Cytotoxicity assays of drug compounds and polymers

Cells were cultured at 37 °C in a dark, humid 5% CO_2 incubator in media containing 1% Pen-Strep, 1% Amphotericin B and supplemented with 10% FCS. For these studies, cells were used between passages 22 and 25. Multiple assays were carried out on ARPE-19 cells to study the effects of different drug concentrations on cell viability, metabolic activity and cell morphology. 18,000 cells/well were seeded in a 48 well tissue culture plate and left for 1 or 7 days to adhere to the plate. The 7 day samples were fed once within the week by replacing 450 μL old medium with 500 μL fresh culture medium. After the predetermined time period, the media was aspirated from all wells and replaced with 0.6 mL fresh media containing polymer blends or controls. Controls included: media, SiO_{1000} (0.2 mL) and a positive control (20 v/v% DMSO in water). Cells were incubated for 1 to 7 days before the following assays could be performed.

Resazurin was dissolved in PBS at 0.1 mg/mL, filtered to make a sterile stock solution and stored at 4 °C in the dark. Medium was removed and replaced with resazurin solution (10 μL stock solution per 100 μL medium). Plates were incubated in the dark at 37 °C for 4 h. Media was removed and put in black 96-well plastic plates; resorufin fluorescence was read using a Fluostar Optima spectrofluorometer ($\lambda_{Excitation}$ = 530 nm; $\lambda_{Emission}$ = 590 nm). All values were normalised to negative control wells on each plate. Finally statistical analysis was performed.

Following removal of resazurin solution, cells were washed with PBS (500 μL) then fixed for 10 min in 10% neutral buffered formalin (NBF; 10% formalin, approximately 4% formaldehyde). NBF was discarded and the cells washed again with PBS. A phalloidin solution was used to stain the F-actin of the cytoskeleton of the cell. A phalloidin solution was produced at 1 mg powder in 1.5 mL MeOH according to manufacturer's instruction. The solution was then diluted 1 in 100 (in fresh PBS) and 75 μL was placed in each well followed by 30 min of incubation at 4 °C. Phalloidin solution was removed and the cells washed with PBS.

DAPI was used to stain the nuclei of the cell. A stock solution of DAPI was made at 1:1000 with PBS, then further diluted to a working solution of 1:10 PBS, 75 μL was placed in each well and incubated for 10 min at 4 °C. Cells were washed with PBS and placed under 500 μL PBS. Cells were then imaged using fluorescence microscopy.

3. Results and discussion

3.1. Drug selection and design of silicone oil-soluble/miscible polymers with potential hydrogen-bonding capability

The use of hydrogen bonding to promote and direct self-assembly in supramolecular systems has been reported for many years [28]; examples include imide-amine [29], amide-amide [30,31], amide-amine [32] and thioamide-thioamide [33] although many other systems have been described. One complementary donor-donor-acceptor-acceptor multiple-hydrogen bonded system, the ureido-pyrimidinone, has been studied in detail since reports of dimerisation were highlighted in non-polar solvents [34]. The introduction of ethylene glycol spacer units within networks of multifunctional ureido-pyrimidones was shown to reduce association within non-polar solvents with a strong correlation to chain length of the incorporated poly(ethylene glycol), (PEG) [35]. Despite this, the use of pH-dependent acid-ether hydrogen-bonding interactions has been reported in the context of controlled colloidal association [36] and emulsion-engineering [37,38] in aqueous environments. The potential for acid-ether hydrogen bonding within a silicone oil environment, therefore, presented an opportunity to moderate the release of acid functional drugs from the tamponade. Two drug classes that have been repeatedly highlighted within recent reviews and reports of ocular research were of interest to this study, namely anti-inflammatory [18,39] and anti-proliferative [40] compounds. The targeted hydrogen bonding interaction was potentially ideal for two specific acid-functional drugs, ibuprofen (Ibu) and all-trans retinoic acid (atRA), as both drugs have been shown in animal models to provide beneficial effects in ocular conditions requiring inflammation and proliferation control respectively [41–45].

The introduction of PEG to silicone oil presents challenges as the water-soluble polymer is practically insoluble within the non-polar silicone oil environment. A series of copolymer structures were designed to overcome this issue and synthesized using the controlled radical polymerization technique reversible addition-fragmentation chain transfer polymerization (RAFT; Scheme 1A) using azobisisobutyronitrile (AIBN) as the free radical initiator. Linear statistical copolymers of the macromonomers oligo(ethyleneglycol) monomethyl ether methacrylate (DP_n = 4 monomer units; OEGMA) and two chain lengths of mono methacryloxypropyl poly(dimethylsiloxane) methacrylate (DP_n = 9 or 57 monomer units; $PDMSMA_{(x)}$) were targeted with an overall number average degree of polymerization (DP_n) = 60 monomer units within the main chain (Scheme 1B). This DP_n value was selected as it was judged to offer a large enough chain length to accommodate a significant number of OEGMA and PDMSMA side chains whilst not developing considerable increases in viscosity after addition to silicone oil. A short OEGMA chain was selected in order to present only a subtle change in the solubility/miscibility of the poly(PDMSMA) linear polymers, and the introduction of either 12 (Scheme 1Bi&ii) or 30 (Scheme 1Biii&iv) units of OEGMA, with both PDMSMA macromonomers, was targeted within the overall DP_n = 60 linear statistical copolymer; this allowed the impact of copolymer composition to be examined within the study.

In addition, a series of branched vinyl polymers were designed to determine any benefits from complex polymer architectures when blended with silicone oil. In our previous work, and work by others, the copolymerisation of a multifunctional vinyl brancher at very low concentration within controlled radical polymerizations has been shown to lead to fully soluble materials with very high molecular weights and comprising multiple primary linear chains [46–54]. The linear chains are not tethered at either of the chain ends, therefore, in any mass of polymer the number of chain ends and the DP_n of the component polymer chains is identical to a corresponding sample of linear polymer prepared in the absence of brancher (Fig. 2); the polymers designed here uniquely utilize a long methacryloxypropyl poly(dimethylsiloxane) dimethacrylate ($PDMSDMA_{(y)}$) branching molecule with varying chain lengths, rather than the often reported small molecule divinyl branchers such as divinyl benzene or ethyleneglycol dimethacrylate.

3.2. Synthesis and characterization of copolymers containing mono methacryloxypropyl poly(dimethylsiloxane) methacrylate and oligo(ethyleneglycol) monomethyl ether methacrylate and their miscibility in silicone oil (SiO_{1000})

The RAFT synthesis of $p(OEGMA_{60})$ in ^{t}BuOH at 70 °C utilized 2-cyano-2-propyl benzodithioate (CPBD) as the chain transfer agent and

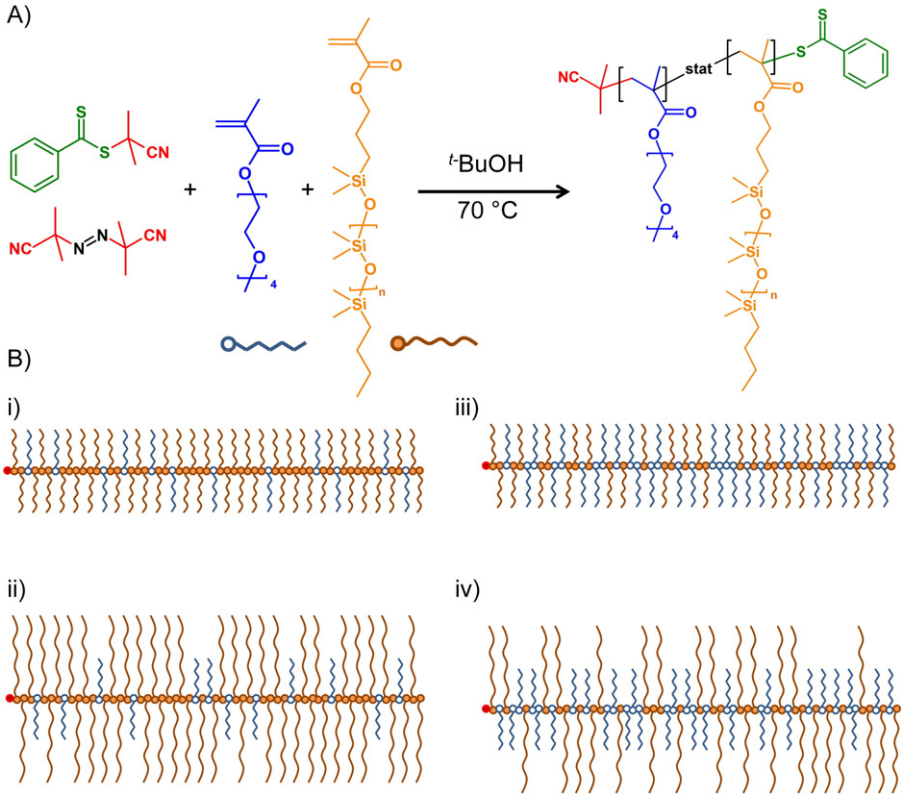

Scheme 1. Synthesis of linear statistical graft copolymers of mono methacryloxypropyl poly(dimethylsiloxane) methacrylate and oligo(ethylene glycol) monomethyl ether methacrylate used during this study. A) Reversible addition-fragmentation chain transfer synthesis; B) Schematic representation of structural and compositional variation within the statistical graft copolymers i) low incorporation of hydrophilic grafts or similar chain length to hydrophobic chains; ii) variation of hydrophobic graft length; iii) increased composition of hydrophilic chains, and iv) increased hydrophobic graft chain length at higher ratios of hydrophilic chains.

was relatively straightforward, achieving >90% conversion of monomer to polymer, accurately targeting the required DP_n and maintaining low dispersity (Table 1). Similarly, the synthesis of $p(PDMSMA_{(x)60})$ homopolymers was also straightforward but required more stringent removal of oxygen from the reaction solution prior to initiation due to its well reported solubility within silicone oils [55]. Polymers with low Đ values and good targeting of molecular weight were achieved when using the relatively short chain length macromonomer (x = 9 repeat units); when the chain length of PDMSMA was increased to DP_n = 57 units, homopolymerization was significantly less successful, achieving only 38% conversion under the same conditions as the previous homopolymer (Table 1). This larger side chain DP_n macromonomer generated

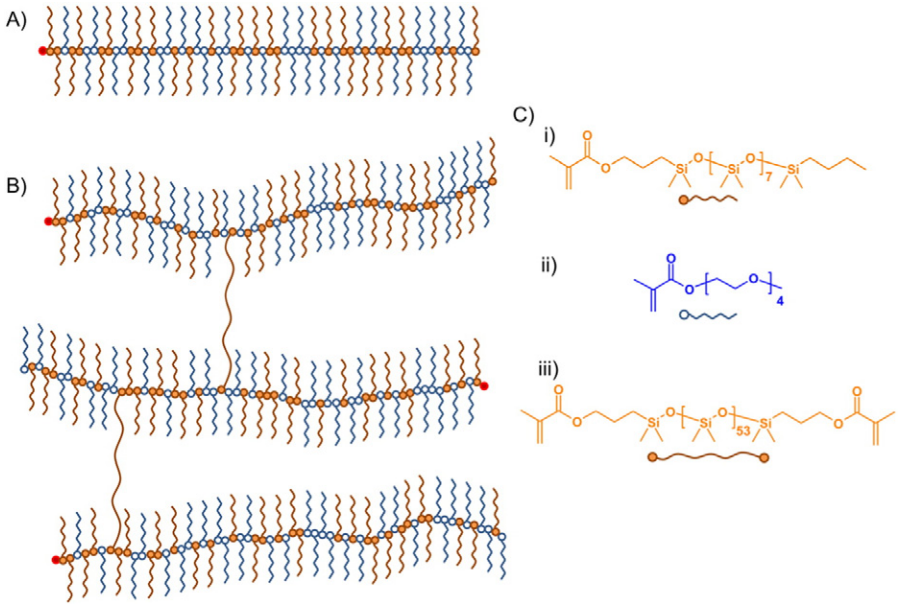

Fig. 2. Schematic representation of polymers and monomers used during the study: A) statistical graft copolymer of mono methacryloxypropyl poly(dimethylsiloxane) methacrylate (Ci) and oligo(ethylene glycol) monomethyl ether methacrylate (Cii); B) branched statistical graft copolymer synthesized using methacryloxypropyl poly(dimethylsiloxane) dimethacrylate (Ciii).

polymers with very high molecular weight and low Đ values despite reaching very low conversion, suggesting a retardation of chain growth, presumably through the increased steric hindrance from the long $PDSMA_{(57)}$ chains.

Statistical copolymerization of OEGMA and $PDMSMA_{(x)}$ at a 1:4 or 1:1 M ratio respectively was successful in generating the required amphiphilic copolymers. The introduction of the short OEGMA monomer was unable to significantly enhance the conversion of the longer $PDMSMA_{(57)}$ macromonomer even at a 1:1 M ratio; however, the statistical copolymers $p(PDMSMA_{(9)48}$-*stat*-$OEGMA_{12})$, $p(PDMSMA_{(9)30}$-*stat*-$OEGMA_{30})$, $p(PDMSMA_{(57)48}$-*stat*-$OEGMA_{12})$ and $p(PDMSMA_{(57)30}$-*stat*-$OEGMA_{30})$ were all recovered with low Đ values (1.08–1.21) and molecular weights ranging from M_n = 33.300–350,600 g/mol. When employing $PDMSMA_{(9)}$ both monomers appeared to be incorporated into the polymers well, however, the polymers derived from $PDMSMA_{(57)}$ were richer in OEGMA than targeted.

The introduction of branching within the various $p(PDMSMA_{(9)n}$-*stat*-$OEGMA_m)$ statistical copolymers was achieved by incorporation of very low concentrations of $PDMSDMA_{(y)}$ (y = DP_n = 12 or 55 monomer units); targeting less than one dimethacrylate brancher per primary chain on average (Fig. 2) to prevent crosslinking. The amount of branching that resulted from the introduction of $PDMSDMA_{(12)}$ at a CTA:brancher molar ratio of 1:0.95 was limited and the resulting polymers maintained M_n values that were similar to the analogous linear polymers synthesized in the absence of brancher; Đ values increased as expected with concomitant increases in M_w. The lack of success within the branching syntheses was presumed to be due to the length of the chosen $PDMSDMA_{(12)}$ brancher being less than double the length of the short $PDMSMA_{(9)}$, hence the interchain steric hindrance generated by side chain overlap would prevent efficient branching between growing chains.

Increasing the chain length of the $PDMSDMA_{(y)}$ brancher from 12 to 55 monomer units was expected to overcome the problem of interchain branching and, indeed, soluble polymers of considerably increased molecular weights were prepared. As with previous reports of branched vinyl polymers using multi-functional branchers, the *stat*istical terpolymer $p(PDMSMA_{(9)48}$-*stat*-$OEGMA_{12}$-*stat*-$PDMSDMA_{(55)0.95})$ can be considered as having a large number of conjoined primary chains that have been shown to be near-identical to polymers synthesized in the absence of brancher. Through simple comparison of the M_n and M_w values of the branched and un-branched polymers, it can be seen that this polymer has an estimated number average of 9 conjoined chains and an estimated weight average of 68 conjoined statistical primary chains. The relevance of the weight average number of chains lies in the recognition that the M_w value approximately represents the molecular weight of the polymer chains at the mid-point of the weight fraction or, in other words, approximately half of the physical mass of the polymer sample is composed of structures with >68 conjoined chains. Similar evaluation of the statistical terpolymer $p(PDMSMA_{(9)30}$-*stat*-$OEGMA_{30}$-*stat*-$PDMSDMA_{(55)0.95})$ shows a material with considerably more branching (number average number of conjoined primary chains = 4; weight average number of conjoined primary chains = 142), again indicating that steric factors are important within the statistical copolymerization and branched terpolymerizations. These estimations do rely on attaining similar conversions of both monomers in the presence and absence of brancher, and the primary chains comprising the branched $p(PDMSMA_{(9)30}$-*stat*-$OEGMA_{30}$-*stat*-$PDMSDMA_{(55)0.95})$ terpolymer may have a slightly higher $PDMSMA_{(9)}$ content, and therefore higher DP_n, M_n and M_w than the linear statistical copolymer analogue.

Comparisons of the size exclusion chromatograms clearly showed an overlap of the refractive index (RI) and right angle light scattering (RALS) signals for the linear statistical graft copolymers and branched statistical graft terpolymers utilizing the shorter $PDMSDMA_{(12)}$ brancher with only slight broadening of the distribution. This is in stark contrast to the comparison of materials synthesized using the $PDMSDMA_{(55)}$ brancher, where a significant broadening was seen using the RI detector and scattering was dominated by the high molecular weight branched material within the RALS signal (see Electronic Supporting Information (ESI), Fig. S2 and S3). To improve the potential for successful branching and increase the amount of PDMS within the polymers, the PDMS monomethacrylate portions of the linear and branched graft copolymers were mixed to allow both long ($PDMSMA_{(57)}$) and short ($PDMSMA_{(9)}$) chains to react into a statistical linear terpolymer. The incorporation of OEGMA was not affected by the additional monomer, however, the overall total molar conversion of $PDMSMA_{(x)}$ was reduced when compared to the linear copolymer analogues (Table 1). When used in branching reactions which utilized only the $PDMSDMA_{(55)}$ brancher, the mixed monomer approach did not considerably enhance the formation of branched polymer structures (Fig. S4), probably due to the steric effects seen with shorter brancher:monomer combinations and the inability of $PDMSDMA_{(55)}$ to bridge between chains containing $PDMSMA_{(57)}$ side chains.

The miscibility/solubility of the copolymer structures with silicone oil (SiO_{1000}, viscosity = 900–1200 cSt) was evaluated qualitatively through blending of the silicone oil with increasing amounts of each

Table 1
Characterization of the synthesized study copolymers.

		GPC[a] (THF)			^{1}H NMR[b]		
						Conversion(%)	
Target polymer composition	Brancher	M_n (g/mol)	M_w (g/mol)	Đ	Polymer composition	PDMS	OEGMA
$p(OEGMA_{60})$	–	24,800	30,400	1.23	$p(OEGMA_{55})$	–	92
$p(PDMSMA_{(9)60})$	–	51,200	59,400	1.16	$p(PDMSMA_{(9)58})$	96	–
$p(PDMSMA_{(57)60})$	–	376,000	439,900	1.17	$p(PDMSMA_{(57)23})$	38	–
$p(PDMSMA_{(9)48}$-*stat*-$OEGMA_{12})$	–	47,650	52,700	1.11	$p(PDMSMA_{(9)47}$-*stat*-$OEGMA_{11})$	98	94
$p(PDMSMA_{(9)30}$-*stat*-$OEGMA_{30})$	–	33,300	36,800	1.11	$p(PDMSMA_{(9)24}$-*stat*-$OEGMA_{29})$	80	96
$p(PDMSMA_{(57)48}$-*stat*-$OEGMA_{12})$	–	350,600	380,200	1.08	$p(PDMSMA_{(57)22}$-*stat*-$OEGMA_9)$	45	77
$p(PDMSMA_{(57)30}$-*stat*-$OEGMA_{30})$	–	220,250	266,850	1.21	$p(PDMSMA_{(57)14}$-*stat*-$OEGMA_{20})$	47	65
$p(PDMSMA_{(9)48}$-*stat*-$OEGMA_{12})$	$PDMS\text{-}DMA_{(12)0.95}$	56,200	74,200	1.32	–	94	98
$p(PDMSMA_{(9)30}$-*stat*-$OEGMA_{30})$	$PDMS\text{-}DMA_{(12)0.95}$	50,700	75,600	1.49	–	91	97
$p(PDMSMA_{(9)48}$-*stat*-$OEGMA_{12})$	$PDMS\text{-}DMA_{(55)0.95}$	423,900	3,590,000	8.47	–	91	98
$p(PDMSMA_{(9)30}$-*stat*-$OEGMA_{30})$	$PDMS\text{-}DMA_{(55)0.95}$	142,100	5,220,000	36.73	–	90	97
$p(PDMSMA_{(9)24}$-*stat*-$PDMSMA_{(57)24}$-*stat*-$OEGMA_{12})$	–	149,700	199,300	1.33	$p(PDMSMA_{(9.57)37}$-*stat*-$OEGMA_{11})$	78	92
$p(PDMSMA_{(9)15}$-*stat*-$PDMSMA_{(57)15}$-*stat*-$OEGMA_{30})$	–	95,400	108,600	1.14	$p(PDMSMA_{(9.57)23}$-*stat*-$OEGMA_{29})$	77	95
$p(PDMSMA_{(9)24}$-*stat*-$PDMSMA_{(57)24}$-*stat*-$OEGMA_{12})$	$PDMS\text{-}DMA_{(55)0.95}$	174,100	389,900	2.24	–	92	89
$p(PDMSMA_{(9)15}$-*stat*-$PDMSMA_{(57)15}$-*stat*-$OEGMA_{30})$	$PDMS\text{-}DMA_{(55)0.95}$	235,600	323,200	1.37	–	79	91

[a] GPC values (M_n, M_w and Đ) were determined using THF eluent at 1 mL min^{-1} flow rate.
[b] ^{1}H NMR measurements conducted in $CDCl_3$ solvent and relative conversion calculated using the peak area ratios of PDMS repeat units (δ = 3.80 ppm) and OEGMA repeat units (δ = 3.30 ppm). See Electronic Supporting Information, (ESI) Fig. S1 for an example of conversion determination.

composition and architecture (Table 2). As a control, the homopolymers $p(OEGMA_{60})$, $p(PDMSMA_{(9)60})$ and $p(PDMSMA_{(57)60})$ were first evaluated and showed almost no solubility of $p(OEGMA_{60})$, as expected, and complete miscibility for both the $p(PDMSMA_{(x)60})$ homopolymers (Table 2). When OEGMA and PDMSMA were statistically copolymerised to incorporate just 12 units of OEGMA within the target DP_{60} polymer chain, and utilizing $PDMSMA_{(9)}$ to form $p(PDMSMA_{(9)48}$-*stat*-$OEGMA_{12})$, the resulting polymer was only miscible at <30 v/v%. A further reduction in miscibility was seen when $p(PDMSMA_{(9)30}$-*stat*-$OEGMA_{30})$ was tested, demonstrating the clearly negative effect of OEGMA on the miscibility of these materials. Increasing the PDMSMA graft length within the same target DP_{60} polymers, and nominal compositions, allowed the polymers $p(PDMSMA_{(57)48}$-*stat*-$OEGMA_{12})$ and $p(PDMSMA_{(57)30}$-*stat*-$OEGMA_{30})$ to overcome the impact of OEGMA incorporation, even when OEGMA comprised 50 mol% of the target polymer backbone repeat units. Due to the poor branching observed when using $PDMSDMA_{(12)}$, terpolymers synthesized using this brancher were not studied; however, very high molecular weight branched statistical terpolymers formed using $PDMSDMA_{(55)}$ exhibited improved miscibility when compared to their linear copolymer analogues, despite only very small modifications of the overall nominal molar ratio of ethylene glycol:dimethyl siloxane units within these samples. The substitution of half of the $PDMSDMA_{(9)}$ with $PDMSDMA_{(57)}$, leading to the synthesis of statistical terpolymers $p(PDMSMA_{(9)24}$-*stat*-$PDMSMA_{(57)24}$-*stat*-$OEGMA_{12})$ and $p(PDMSMA_{(9)15}$-*stat*-$PDMSMA_{(57)15}$-*stat*-$OEGMA_{30})$, resulted in a large impact on miscibility as expected. It is interesting to note that within the linear copolymer and terpolymer samples, high miscibility was only achievable when $PDMSMA_{(57)}$ was present with a concomitant large decrease in the molar content of ethylene glycol repeat units in the targeted polymers to approximately ≤10 mol% (Table 2). The introduction of less than one $PDMSDMA_{(55)}$ brancher per primary chain, therefore, allowed a considerable increase in the molar content of ethylene glycol that could be incorporated into the silicone oil/polymer mixture, potentially due to the formation of micelle-like nanostructures; this was not further investigated within this study.

To establish the benefits of the silicone oil/graft statistical copolymer mixtures in tamponade drug reservoir applications, the residual polymer colour resulting from RAFT polymerization was first removed by cleavage of the remaining dithioester chain end groups. A single polymer was selected for this modification and subsequent drug release studies, namely $p(PDMSMA_{(9)48}$-*stat*-$OEGMA_{12})$. Polymer selection criteria included ease/lack of complexity of synthesis, miscibility with silicone oil and the relatively low ethylene glycol content within the final polymer; high levels of $p(OEGMA)$ may allow the incorporation of significant water levels within the silicone oil tamponade and this is known to lead to a decrease of optical clarity over time through emulsion formation. Removal of the residual chain transfer agent was accomplished by using a previously reported approach [56] involving treatment with AIBN in toluene at 80 °C for 2.5 h, after which a colourless material (Scheme S1) was recovered and analyzed to confirm no change in molecular weight had occurred and the chain end functionality had been completely removed (Fig. S5).

3.3. Cytotoxicty of $p(PDMSMA_{(9)48}$-*stat*-$OEGMA_{12})$ with ARPE-19 cells

The metabolic activity and morphology of ARPE-19 cells, a human retinal pigment epithelial cell line [57], was studied as they contain the same functional and structural properties of cell *in vivo*. Both pre- and post-confluent cells (1 day and 7 day growth respectively) were exposed to silicone oil (SiO_{1000}) and blends of $p(PDMSMA_{(9)48}$-*stat*-$OEGMA_{12})$ with silicone oil at 10 v/v% for 1 and 7 days; a resazurin assay was conducted, followed by phalloidin staining of the cells from the assay. The resazurin assay contained negative (healthy cells) and positive controls (cells exposed to 20% DMSO) as well as media with no resazurin present to determine background signals. The controls confirmed the validity of the assay (Fig. 3), as there was a significant difference ($p \leq 0.05$) between the negative control and the positive control, however, no significant difference ($p \leq 0.05$) was observed between the positive control and cells exposed to silicone oil or $p(PDMSMA_{(9)48}$-*stat*-$OEGMA_{12})$ blends at 10 v/v% in silicone oil, indicating that the oil and blends have no measurable effect on the metabolic activity of the ARPE-19 cells.

Phalloidin and DAPI staining confirmed the presence of attached cells that were well-spread with typical actin stress fiber structures when exposed to the oil and polymer blend. Images of phalloidin-stained cells exposed to silicone oil, and the 10 v/v% blends alongside negative control (healthy cells) for the two extreme time points examined (Fig. 4), and measurement of metabolic activity indicate that the oils and polymer blend are non-cytotoxic to this cell type.

3.4. Controlling in vitro release of ibuprofen and all-trans retinoic acid from tamponade blends containing silicone oil and $p(PDMSMA_{(9)48}$-*stat*-$OEGMA_{12})$

As discussed above, blends of silicone oil and $p(PDMSMA_{(9)48}$-*stat*-$OEGMA_{12})$ were targeted to regulate the long term release of acid-functional drugs due to the potential for hydrogen bonding with the ethylene glycol repeat units solubilised within the non-polar environment of the silicone oil (Fig. 5). The measurement of drug release from silicone oil has been previously described using various methods such as studying depletion from the oil phase and employing a range of extraction techniques with organic solvents to allow subsequent UV–visible spectroscopy to quantify concentrations, often *via* high pressure liquid chromatography [58].

These techniques have considerable scope for inaccuracy and have limited value when measuring release into cell culture media; direct measurement of atRA and Ibu in culture media is hampered by an

Table 2
Results of statistical graft homopolymer, copolymer and terpolymer/silicone oil miscibility studies and target mole% of PDMS and ethylene glycol repeat units.

Target Polymer	Brancher	Target composition (mol% of total monomer)		Miscibility in Silicone Oil
Composition		EG	DMS	(% v/v)
$p(OEGMA_{60})$	–	100	0	<1
$p(PDMSMA_{(9)60})$	–	0	100	Miscible
$p(PDMSMA_{(57)60})$	–	0	100	Miscible
$p(PDMSMA_{(9)48}$-*stat*-$OEGMA_{12})$	–	10	90	<30
$p(PDMSMA_{(9)30}$-*stat*-$OEGMA_{30})$	–	30.8	69.2	<5
$p(PDMSMA_{(57)48}$-*stat*-$OEGMA_{12})$	–	1.7	98.3	Miscible
$p(PDMSMA_{(57)30}$-*stat*-$OEGMA_{30})$	–	6.5	93.5	Miscible
$p(PDMSMA_{(9)48}$-*stat*-$OEGMA_{12})$	$PDMSDMA_{(55)}$	9	91	<40
$p(PDMSMA_{(9)30}$-*stat*-$OEGMA_{30})$	$PDMSDMA_{(55)}$	27	73	<40
$p(PDMSMA_{(9)24}$-*stat*-$PDMSMA_{(57)24}$-*stat*-$OEGMA_{12})$	–	2.9	97.1	Miscible
$p(PDMSMA_{(9)15}$-*stat*-$PDMSMA_{(57)15}$-*stat*-$OEGMA_{30})$	–	10.8	89.2	Miscible

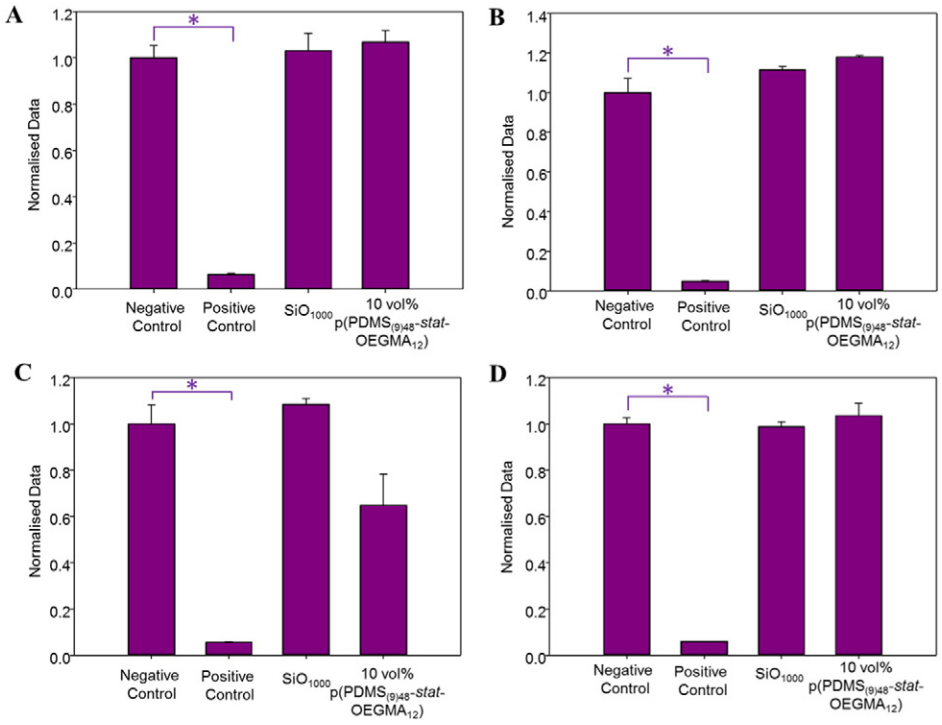

Fig. 3. Resazurin assay with appropriate controls to determine the cytotoxicity of silicone oil (SiO_{1000}) and blends of $p(PDMSMA_{(9)48}$-*stat*-$OEGMA_{12})$ with silicone oil (SiO_{1000}) at 10 v/v%. Pre- and post-confluent ARPE-19 cells (grown for 1 and 7 days respectively) were exposed to the oils for 1 and 7 d. A: Pre-confluent cells exposed for 1 day, B: Post-confluent cells exposed for 7 days, C: Pre-confluent cells exposed for 7 days and D: Post-confluent cells exposed for 1 day. (mean, error bars represent ±1 standard deviation); $n = 3$. *, Significance by ANOVA and Dunnett's T3 post-hoc evaluation ($p \leq 0.05$).

overlap of drug and the absorption peaks of the media components, such as fetal calf serum (Fig. S7). Our attempts to accurately quantify the concentration of drugs in silicone oil directly by ^{1}H nuclear magnetic resonance spectroscopy of the oil were also impeded by their reported low solubility in this liquid. To overcome these issues, mixtures of drug compounds with relatively low ratios of radiolabelled drugs (^{3}H-Ibu and ^{3}H-atRA) were employed, allowing direct measurement of samples containing very low drug concentrations without subsequent manipulation and additional error. Additionally, ^{3}H-labelled drugs are essentially unchanged chemically and the use of techniques to amplify detection that require conjugation of fluorophores are avoided.

Initial release studies into media were conducted using ^{3}H-Ibu/Ibu mixtures dissolved at a concentration of 1 mg/mL (specific activity ranging from 1.39–1.61 μCi/μg across different experiments) either in silicone oil or a blend of silicone oil and $p(PDMSMA_{(9)48}$-*stat*-$OEGMA_{12})$ at 5 or 10 v/v% addition of copolymer (Fig. 6A).

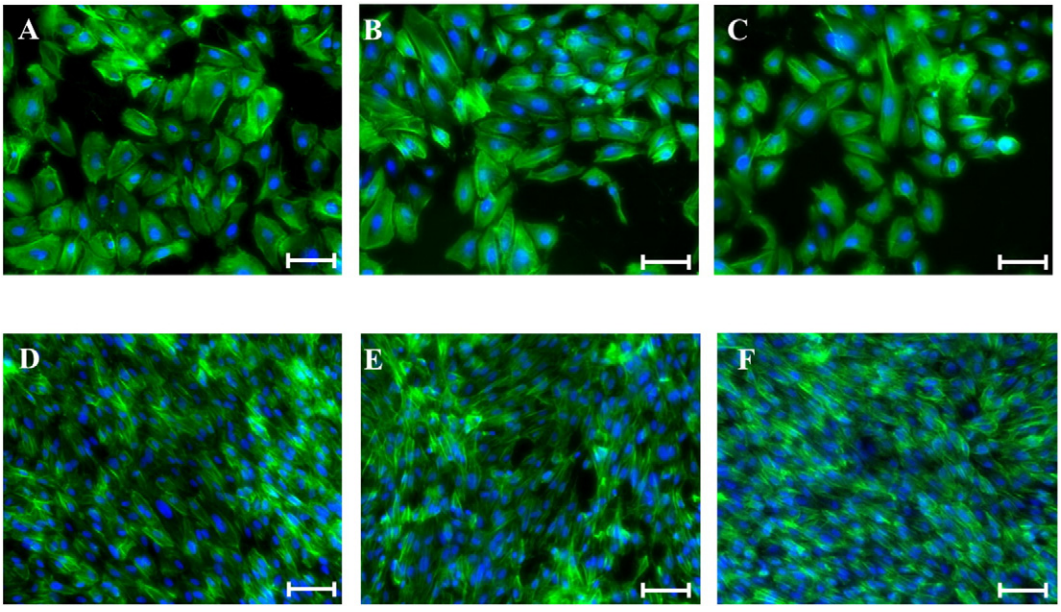

Fig. 4. ARPE-19 cells stained with phalloidin (green, F-actin cytoskeleton) and DAPI (blue, nuclei). Pre-confluent cells: A)Negative control; B) Exposed to silicone oil (SiO_{1000}); C) Exposed to a 10 v/v% blend of $p(PDMSMA_{(9)48}$-*stat*-$OEGMA_{12})$ for 1 day; and post-confluent cells: D) Negative control; E), Exposed to silicone oil (SiO_{1000}); F) Exposed to a 10 v/v% blend of $p(PDMSMA_{(9)48}$-*stat*-$OEGMA_{12})$ for 7 days. Scale bars represent 50 μm. Additional timescales studied; see Fig. S6.

In the absence of the statistical graft copolymer, the release of Ibu from silicone oil was initially very rapid with approximately 65% of the dissolved drug released in the first day of the experiment; complete release of drug occurred after 3 days under the conditions described above. The inclusion of 5 v/v% of *p*(PDMSMA$_{(9)48}$-*stat*-OEGMA$_{12}$) noticeably reduced the rate of Ibu release, extending the release to between 6 and 7 days whilst the inclusion of 10 v/v% of the copolymer slowed the release of Ibu to <50 wt% over the first day and extending the release for over 1 week. The additional reduction in release rate observed at the higher inclusion rate of the copolymer suggests that a significant amount of Ibu remained unbound within the sample containing 5 v/v% statistical graft copolymer.

The experiment was repeated using ^{3}H-atRA/atRA mixtures but due to the reported low solubility of atRA in silicone oil [58], a concentration of 20 μg/mL was employed. As seen with the Ibu release from silicone oil, the absence of copolymer allowed a relatively fast release of drug (>60%) within 3 days and 80% release was seen after 9 days (Fig. 6B). Within a clinical setting, the release of atRA would ideally be sustained over several months, therefore monitoring was conducted for extended periods. The inclusion of 5 and 10 v/v% of *p*(PDMSMA$_{(9)48}$-*stat*-OEGMA$_{12}$) led to the same effect observed for Ibu; that the addition of the statistical graft copolymer retarded the release of the acid-functional drug. In this case, however, the difference between the two statistical graft copolymer inclusion levels was very small over the 72 day sampling period, with both systems reaching 80% release at approximately 40 days. This approximate 4-fold delay in release of atRA may offer considerable clinical benefit, potentially enabling dosing from the silicone oil tamponade drug reservoir to be maintained within therapeutic limits. The concentration of the ^{3}H-atRA/atRA mixture was increased to 200 μg/mL and identical release studies were undertaken (Fig. 6C). As observed at the lower atRA concentration, the absence of statistical graft copolymer led to a rapid release over the first 4 days (>60 wt%) and the inclusion of 5 v/v% of *p*(PDMSMA$_{(9)48}$-*stat*-OEGMA$_{12}$) led to a reduction in release rate. Interestingly, under these conditions, the addition of 10 v/v% of the statistical graft copolymer did lead to a further retardation of release at this higher concentration of drug; with the three conditions reaching nearly 100% release in approximately 50 days in the absence of statistical graft copolymer, and 95% and 90% release after 72 days in the presence of 5 v/v% and 10 v/v% copolymer respectively. This strongly suggests that the inclusion of 5 v/v% of *p*(PDMSMA$_{(9)48}$-*stat*-OEGMA$_{12}$) within the silicone oil at a atRA concentration of 20 μg/mL had resulted in the binding of almost all of the drug to the polymer OEGMA sites and the addition of further OEGMA was unnecessary; however, at higher atRA concentrations (200 μg/mL), the increased retardation seen from a doubling of the copolymer addition would suggest that the copolymer was predominantly saturated at an inclusion rate of 5 v/v%. Even under conditions where the polymer binding sites are saturated, the difference in release rate with different copolymer inclusion is noticeable at the first measurement (day 1) where the absence of copolymer at an atRA concentration of 20 μg/mL led to approximately 35% release and the presence of copolymer at 5 v/v% and 10 v/v% reduced the release to a measured 20% and 18% respectively. At the higher atRA concentration of 200 μg/mL, the values after 1 day were approximately 20%, 16% and 15% for the absence and inclusion of copolymer at 5 v/v% and 10 v/v% respectively.

4. Conclusions

A vitrectomy and subsequent replacement of the vitreous humour with a silicone oil tamponade is a critical tool in the clinical management of many cases of retinal detachment and the opportunity to utilize the tamponade as a drug delivery reservoir has been an elusive target for many years. Low drug solubilities and poor control of drug release are two key factors in the lack of clinical therapeutic tamponade options. The bespoke design of silicone oil-soluble polymer excipients to enhance solubility and mediate drug release is an area with considerable options and one that appears to have been largely unstudied. To the best of our knowledge, the use of PEG-containing silicone-oil soluble/miscible polymers to control drug release in an ophthalmic setting has not been reported previously, but the results herein suggest new avenues for this area of drug delivery research. The polymer chosen for detailed study was selected based on its simplicity, both of synthesis and architecture, and represents an option with clear translational potential. By selecting to target acid-functional drug compounds, we have also demonstrated the ability to enable anti-inflammatory drug release over a 1 week period and the sustained release of an anti-proliferative drug over several months. This may be important to counteract the immediate effects of damage and prevent further injury during the recovery stages. This strategy offers new approaches to enable clinicians in their prevention of sight loss and to aid patients during their recovery from retinal detachment.

Author contributions

The manuscript was written through contributions of all authors. All authors have given approval to the final version of the manuscript.

Conflict of interest

The authors are co-inventors of a recently filed patent application that describes the work reported here.

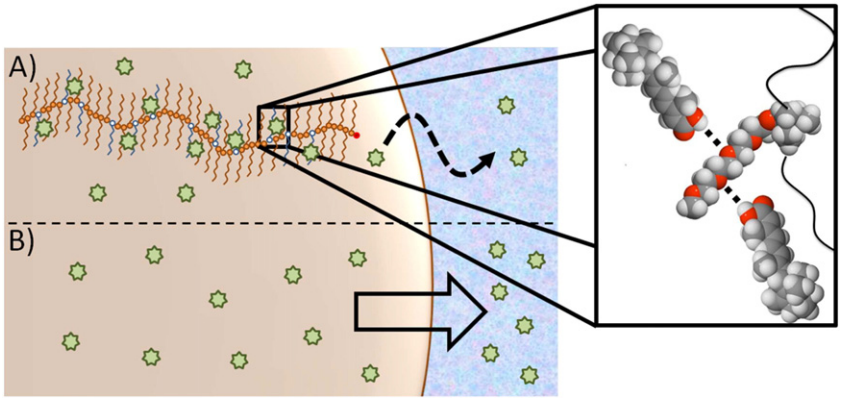

Fig. 5. Schematic representation of silicone oil-aqueous media interface: A) drug molecules *co*-dissolved within the silicone oil with the statistical graft copolymer of mono methacryloxypropyl poly(dimethylsiloxane) methacrylate polydimethylsiloxane methacrylate and oligo(ethyleneglycol) monomethyl ether methacrylate and hydrogen bonding to the ethylene glycol repeat units leading to slow release of drug; B) drug dissolved solely within the silicone oil phase, leading to rapid release. Inset shows the potential hydrogen bonding between acid functional drugs and the ethylene glycol units within the statistical graft copolymer.

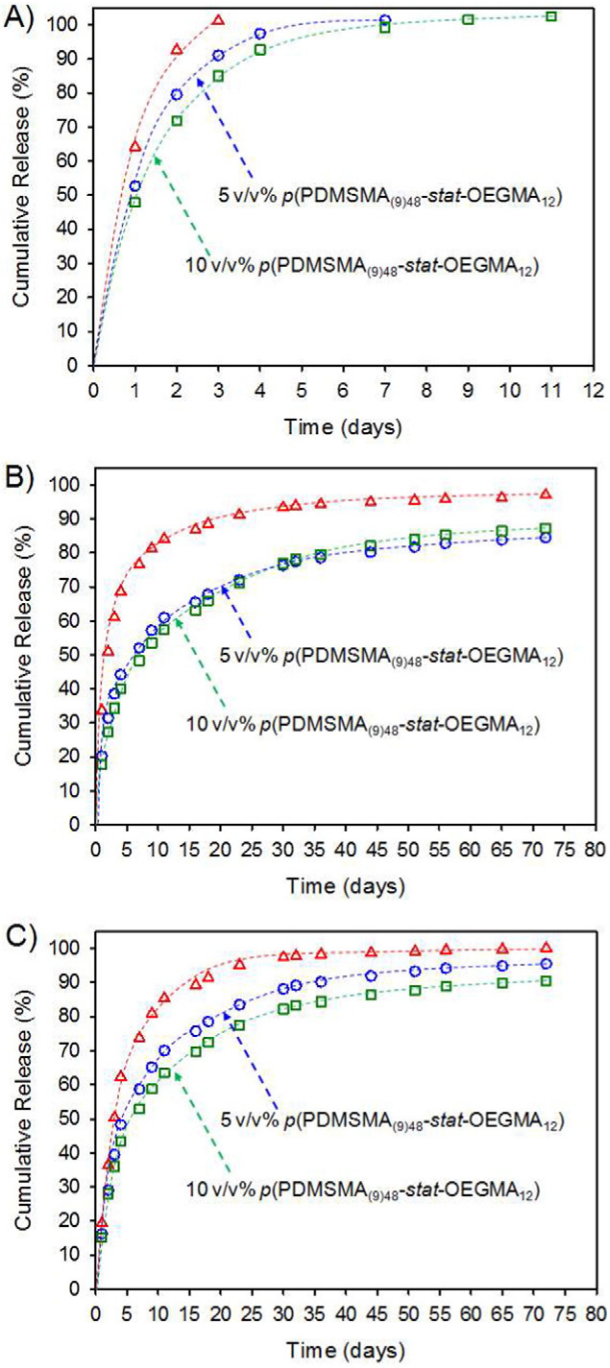

Fig. 6. Studies of acid-functional drug release from silicone oil tamponades into aqueous media in the absence (open red triangles) and presence of statistical graft copolymer, using drug mixtures containing ^{3}H-labelled compounds. **Ibuprofen release:** A) Effect of increasing dissolved graft copolymer within the blend from 5 v/v% (open blue circles) to 10 v/v% (open green squares) - 1 mg/mL ibuprofen within the silicone oil phase. **all-trans Retionoic acid release:** Effect of increasing dissolved graft copolymer from 5 v/v% (open blue circles) to 10 v/v% (open green squares) within the silicone oil at all-trans retinoic acid concentrations of B) 20 μg/mL, and C) 200 μg/mL.

Acknowledgment and funding sources

The authors are grateful for funding provided by the Engineering and Physical Sciences Research Council (EP/L000458/1, EP/M002209/1, EP/L02635X/1 and EP/I038721/1) and for a PhD studentship from the University of Liverpool (HC). We also acknowledge the Centre for Materials Discovery for access to essential equipment, Fluoron GmbH for donation of silicone oil and Mr Theodor Stappler for advice on clinical aspects.

Appendix A. Supplementary data

^{1}H NMR spectra, gel permeation chromatograms, cell imaging, UV spectra and figures of samples. This material is available free of charge *via* the Internet at http://pubs.acs.org. Supplementary data associated with this article can be found in the online version at http://dx.doi.org/10.1016/j.jconrel.2016.11.010.

References

[1] H. Abouzeid, T.J. Wolfensberger, Macular recovery after retinal detachment, Acta Ophthalmol. Scand. 84 (2006) 597–605.
[2] M. Ivanišević, L. Bojić, D. Eterović, Epidemiological study of non-traumatic phakic rhegmatogenous retinal detachment, Ophthalmic Res. 32 (2000) 237–239.
[3] S. Go, C.B. Hoyng, C.W. Klaver, Genetic risk of rhegmatogenous retinal detachment: a familial aggregation study, Arch. Ophthalmol. 123 (2005) 1237–1241.
[4] C.-C. Lai, Y.-P. Chen, N.-K. Wang, L. Liu, K.-J. Chen, Y.-S. Hwang, W.-C. Wu, T.-L. Chen, L.-H. Chuang, Vitrectomy with internal limiting membrane repositioning and autologous blood for macular hole retinal detachment in highly myopic eyes, Ophthalmology 122 (2015) 1889–1898.
[5] V. Daien, A. Le Pape, D. Heve, I. Carriere, M. Villain, Incidence, risk factors, and impact of age on retinal detachment after cataract surgery in France: a national population study, Ophthalmology 122 (2015) 2179–2185.
[6] M.A.J. Van de Put, J.M.M. Hooymans, L.I. Los, The incidence of rhegmatogenous retinal detachment in the Netherlands, Ophthalmology 120 (2013) 616–622.
[7] H.K. Kang, A.J. Luff, Management of retinal detachment: a guide for non-ophthalmologists, BMJ 336 (2008) 1235–1240.
[8] S. Pennock, L.J. Haddock, D. Eliott, S. Mukai, A. Kazlauskas, Is neutralizing vitreal growth factors a viable strategy to prevent proliferative vitreoretinopathy? Prog. Retin. Eye Res. 40 (2014) 16–34.
[9] J.G. Garweg, C. Tappeiner, M. Halberstadt, Pathophysiology of proliferative vitreoretinopathy in retinal detachment, Surv. Ophthalmol. 58 (2013) 321–329.
[10] A. Sadaka, G.P. Giuliari, Proliferative vitreoretinopathy: current and emerging treatments, Clin. Ophthalmol. 6 (2012) 1325–1333.
[11] C. Chiba, The retinal pigment epithelium: an important player of retinal disorders and regeneration, Exp. Eye Res. 123 (2014) 107–114.
[12] C.K. Chan, S.G. Lin, A.S. Nuthi, D.M. Salib, Pneumatic retinopexy for the repair of retinal detachments: a comprehensive review (1986–2007), Surv. Ophthalmol. 53 (2008) 443–478.
[13] S.G. Schwartz, D.P. Kuhl, A.R. McPherson, E.R. Holz, W.F. Mieler, Twenty-year follow-up for scleral buckling, Arch. Ophthalmol. 120 (2002) 325–329.
[14] T. Banaee, S.M. Hosseini, H. Ghooshkhanei, M. Moosavi, S.J. Khayyatzadeh-Kakhki, Anatomical and visual outcomes of three different scleral buckling techniques, J. Ophthalmic Vis. Res. 4 (2009) 90–96.
[15] A.K.H. Kwok, T.Y.Y. Lai, W.W.K. Yip, Vitrectomy and gas tamponade without internal limiting membrane peeling for myopic foveoschisis, Brit. J. Ophthalmol. 89 (2005) 1180–1183.
[16] M.H. Goldbaum, B.W. McCuen, A.M. Hanneken, S.K. Burgess, H.H. Chen, Silicone oil tamponade to seal macular holes without position restrictions, Ophthalmology 105 (1998) 2140–2147.
[17] Y.-D. Shen, C.-M. Yang, Extended silicone oil tamponade in primary vitrectomy for complex retinal detachment in proliferative diabetic retinopathy: a long-term follow-up study, Eur. J. Ophthalmol. 17 (2007) 954–960.
[18] M.T. Kralinger, U. Stolba, M. Velikay, S. Egger, S. Binder, A. Wedrich, A. Haas, J.-M. Parel, G.F. Kieselbach, Safety and feasibility of a novel intravitreal tamponade using a silicone oil/acetyl-salicylic acid suspension for proliferative vitreoretinopathy: first results of the Austrian Clinical Multicenter Study, Graefes Arch. Clin. Exp. Ophthalmol. 248 (2010) 1193–1198.
[19] K. Park, Drug delivery research: the invention cycle, Mol. Pharm. 13 (2016) 2143–2147.
[20] H. Chen, Recent developments in ocular drug delivery, J. Drug Target. 23 (2015) 597–604.
[21] N. Kamaly, B. Yameen, J. Wu, O.C. Farokhzad, Degradable controlled-release polymers and polymeric nanoparticles: mechanisms of controlling drug release, Chem. Rev. 116 (2016) 2602–2663.
[22] S. Wang, P. Huang, X. Chen, Stimuli-responsive programmed specific targeting in nanomedicine, ACS Nano 10 (2016) 2991–2994.
[23] B.S. Sekhon, Supramolecular nanomedicine - an overview, Curr. Drug Targets 16 (2015) 1407–1428.
[24] M.J. Webber, E.A. Appel, E.W. Meijer, R. Langer, Supramolecular biomaterials, Nat. Mater. 15 (2016) 13–26.
[25] H. Xu, P. Yang, X. Zhang, X. Wu, W. Yin, H. Wang, D. Xu, H. Ma, Targeted polymer-drug conjugates: current progress and future perspective, Colloids Surf. B Biointerfaces 136 (2015) 729–734.
[26] Paramjot, N.M. Khan, H. Kapahi, S. Kumar, T.R. Bhardwaj, S. Arora, N. Mishra, Role of polymer-drug conjugates in organ-specific delivery systems, J. Drug Target. 23 (2015) 387–416.

[27] C.E. Willoughby, D. Ponzin, S. Ferrari, A. Lobo, K. Landau, Y. Omidi, Anatomy and physiology of the human eye: effects of mucopolysaccharidoses disease on structure and function – a review, Clin. Exp. Ophthalmol. 38 (2010) 2–11.
[28] K.A. Houton, A.J. Wilson, Hydrogen-bonded supramolecular polyurethanes, Polym. Int. 64 (2015) 165–173.
[29] A.G. Slater, L.M.A. Perdigão, P.H. Beton, N.R. Champness, Surface-based supramolecular chemistry using hydrogen bonds, Acc. Chem. Res. 47 (2014) 3417–3427.
[30] T. Mes, M.M.J. Smulders, A.R.A. Palmans, E.W. Meijer, Hydrogen-bond engineering in supramolecular polymers: polarity influence on the self-assembly of benzene-1,3,5-tricarboxamides, Macromolecules 43 (2010) 1981–1991.
[31] M. Rajeswara Rao, S.-S. Sun, Supramolecular assemblies of amide-derived organogels featuring rigid π conjugated phenylethynyl frameworks, Langmuir 29 (2013) 15146–15158.
[32] L.M. Pitet, A.H.M. van Loon, E.J. Kramer, C.J. Hawker, E.W. Meijer, Nanostructured supramolecular block copolymers based on polydimethylsiloxane and polylactide, ACS Macro Lett. 2 (2013) 1006–1010.
[33] T. Mes, S. Cantekin, D.W.R. Balkenende, M.M.M. Frissen, M.A.J. Gillissen, B.F.M. De Waal, I.K. Voets, E.W. Meijer, A.R.A. Palmans, Thioamides: versatile bonds to induce directional and cooperative hydrogen bonding in supramolecular polymers, Chem. Eur. J. 19 (2013) 8642–8649.
[34] F.H. Beijer, R.P. Sijbesma, H. Kooijman, A.L. Spek, E.W. Meijer, Strong dimerization of ureidopyrimidones via quadruple hydrogen bonding, J. Am. Chem. Soc. 120 (1998) 6761–6769.
[35] T.F.A. de Greef, M.M.L. Nieuwenhuizen, P.J.M. Stals, C.F.C. Fitié, A.R.A. Palmans, R.P. Sijbesma, E.W. Meijer, The influence of ethylene glycol chains on the thermodynamics of hydrogen-bonded supramolecular assemblies in apolar solvents, Chem. Commun. 4306–4308 (2008).
[36] P. Starck, W.A. Ducker, Simple method for controlled association of colloidal-particle mixtures using ph-dependent hydrogen bonding, Langmuir 25 (2009) 2114–2120.
[37] J.V.M. Weaver, S.P. Rannard, A.I. Cooper, Polymer-mediated hierarchical and reversible emulsion droplet assembly, Angew. Chem. Int. Ed. 121 (2009) 2165–2168.
[38] R.T. Woodward, R.A. Slater, S. Higgins, S.P. Rannard, A.I. Cooper, B.J.L. Royles, P.H. Findlay, J.V.M. Weaver, Controlling responsive emulsion properties via polymer design, Chem. Commun. (2009) 3554–3556.
[39] M.A. Khan, C.J. Brady, R.S. Kaiser, Clinical management of proliferative vitreoretinopathy: an update, Retina 35 (2015) 165–175.
[40] E.G. Heimsath, R. Unda, E. Vidro, A. Muniz, E.T. Villazana-Espinoza, A. Tsin, ARPE-19 cell growth and cell functions in euglycemic culture media, Curr. Eye Res. 31 (2006) 1073–1080.
[41] M.E. Tilden, R.S. Boney, M.M. Goldenberg, J.T. Rosenbaum, The effects of topical s(+)-ibuprofen on interleukin-1 induced ocular inflammation in a rabbit model, J. Ocul. Pharmacol. Ther. 6 (2009) 131–135.
[42] G.W.A. Tjebbes, J.L. van Delft, E.R. Barthen, N.J. van Haeringen, d-Ibuprofen in ocular inflammation induced by paracentesis of the rabbit eye, Prostaglandins 40 (1990) 29–33.
[43] M. Nakagawa, M.F. Refojo, J.F. Marin, M. Doi, F.I. Tolentino, Retinoic acid in silicone and silicone-fluorosilicone copolymer oils in a rabbit model of proliferative vitreoretinopathy, Invest. Ophthalmol. Vis. Sci. 36 (1995) 2388–2395.
[44] W.-C. Wu, D.-N. Hu, S. Mehta, Y.-C. Chang, Effects of retinoic acid on retinal pigment epithelium from excised membranes from proliferative vitreoretinopathy, J. Ocul. Pharmacol. Th. 21 (2005) 44–54.
[45] J.W. Doyle, R.K. Dowgiert, S.M. Buzney, Factors modulating the effect of retinoids on cultured retinal pigment epithelial cell proliferation, Curr. Eye Res. 11 (1992) 753–765.
[46] N.M.B. Smeets, Amphiphilic hyperbranched polymers from the copolymerization of a vinyl and divinyl monomer: the potential of catalytic chain transfer polymerization, Eur. Polym. J. 49 (2013) 2528–2544.
[47] I. Bannister, N.C. Billingham, S.P. Armes, S.P. Rannard, P. Findlay, Development of branching in living radical copolymerization of vinyl and divinyl monomers, Macromolecules 39 (2006) 7483–7492.
[48] T. He, D.J. Adams, M.F. Butler, A.I. Cooper, S.P. Rannard, Polymer nanoparticles: shape-directed monomer-to-particle synthesis, J. Am. Chem. Soc. 131 (2009) 1495–1501.
[49] I. Bannister, N.C. Billingham, S.P. Armes, Monte Carlo modelling of living branching copolymerisation of monovinyl and divinyl monomers: comparison of simulated and experimental data for ATRP copolymerisation of methacrylic monomers, Soft Matter 5 (2009) 3495–3504.
[50] Y. Li, S.P. Armes, Synthesis of branched water-soluble vinyl polymers via oxyanionic polymerization, Macromolecules 38 (2005) 5002–5009.
[51] R.A. Slater, T.O. McDonald, D.J. Adams, E.R. Draper, J.V.M. Weaver, S.P. Rannard, Architecture-driven aqueous stability of hydrophobic, branched polymer nanoparticles prepared by rapid nanoprecipitation, Soft Matter 8 (2012) 9816–9827.
[52] F.L. Hatton, P. Chambon, T.O. McDonald, A. Owen, S.P. Rannard, Hyperbranched polydendrons: a new controlled macromolecular architecture with self-assembly in water and organic solvents, Chem. Sci. 5 (2014) 1844–1853.
[53] F.L. Hatton, L.M. Tatham, L.R. Tidbury, P. Chambon, T. He, A. Owen, S.P. Rannard, Hyperbranched polydendrons: a new nanomaterials platform with tuneable permeation through model gut epithelium, Chem. Sci. 6 (2015) 326–334.
[54] F.L. Hatton, P. Chambon, A.C. Savage, S.P. Rannard, Role of highly branched, high molecular weight polymer structures in directing uniform polymer particle formation during nanoprecipitation Chem, Communications 52 (2016) 3915–3918.
[55] R. Rodnight, Manometric determination of the solubility of oxygen in liquid paraffin, olive oil and silicone fluids, Biochem. J. 57 (1954) 661–663.
[56] S. Perrier, P. Takolpuckdee, C.A. Mars, Reversible addition-fragmentation chain transfer polymerization: end group modification for functionalized polymers and chain transfer agent recovery, Macromolecules 38 (2005) 2033–2036.
[57] K.C. Dunn, A.E. Aotaki-Keen, F.R. Putkey, L.M. Hjelmeland, ARPE-19, a human retinal pigment epithelial cell line with differentiated properties, Exp. Eye Res. 62 (2) (1996 Feb) 155–169.
[58] J.J. Araiz, M.F. Refojo, M.H. Arroyo, F.L. Leong, D.M. Albert, F.I. Tolentino, Antiproliferative effect of retinoic acid in intravitreous silicone oil in an animal model of proliferative vitreoretinopathy, Invest. Ophthalmol. Vis. Sci. 34 (1993) 522–530.